Comparing the Performance of Different Classifiers for Urban Change Detection: A Case Study in Kingston, Ontario

Masoud Babadi Ataabadi [1], Dongmei Chen [1], Darren Pouliot [2], Temitope Seun Oluwadare [1]

[1] Laboratory of Geographic Information and Spatial Analysis, Department of Geography and Planning, Queen's University, Kingston, ON K7L 3N6, Canada – (22mba1, chendm, oluwadare.t)@queensu.ca
[2] Landscape Science and Technology Division, Environment and Climate Change Canada, Ottawa, ON K1A0H3, Canada – darren.pouliot@ec.gc.ca

Keywords: Urban Change Detection, Classifier Performance, Post-Classification, Difference Image Classification, High Resolution Satellite Images.

Abstract

Remote Sensing-based change detection (CD) focuses on the identification of Earth's surface transformations through analysis of multi-temporal satellite images captured for the same geographic region at different points in time. Two common classification-based change detection techniques are post-classification comparison of land cover maps and direct classification of image differences between two periods of interest. In either approach, the selection of an appropriate classifier is critical. Consequently, this study focuses on assessing the performance of different classifiers, including the multi-layer perceptron neural network (MLPNN), support vector machine (SVM), random forest (RF), maximum likelihood (MLH), k-nearest neighbor (KNN), and gaussian naïve bayes (GNB). For this evaluation, two high resolution images captured in 2016 and 2020 by the PS2 sensor within the PlanetScope satellite constellation were used. Additionally, a novel unbiased sampling technique was introduced to selectively capture a minimal number of reference pixels. In the context of change detection, slight variations were observed in classification performance rankings between post-classification and difference image classification methods. However, a consistent trend emerged. The MLPNN consistently achieved the highest accuracy, closely followed by RF and SVM as the second or third-best performers in each technique. In contrast, GNB consistently yielded less favourable results. Importantly, our findings highlight the persistent superiority of the difference image classification in terms of change detection accuracy across all six classifiers. Furthermore, this method offers a significant advantage due to its reduced processing time and computational demands, positioning it as the preferred choice for binary change detection when compared to post-classification techniques.

1. Introduction

The earth's surface is rapidly changing due to the dynamic and evolving nature of ecosystems and the acceleration of the human transformation of nature (Li et al., 2017). Thus, accurate access to surface change data is crucial for improving land management, protecting the ecological environment, and understanding the interactions and relationships between human life and the environment (Tan et al., 2019). Aiming to identify changes in the Earth's surface over time, change detection (CD) is an important field of study in remote sensing by the analysis of multi-temporal satellite images captured for the same geographical area at different times. Change detection has a wide range of applications, including monitoring urban development, deforestation, natural disasters, etc. (Daudt et al., 2018; Khan et al., 2017; Usman et al., 2015; Mucher et al., 2000).

Many techniques and methodologies have been developed for change detection using remotely sensed data and newer techniques are still emerging. These techniques can be categorized differently based on different viewpoints (Hussain et al., 2013). A common grouping is unsupervised and supervised CD techniques (Fernandez-Prieto and Marconcini, 2011). Unsupervised change detection refers to a set of methods that can identify changes entirely driven from the input data without the use of predefined labeled trained data (Bovolo et al., 2011). Supervised methods require labeled training examples as a basis for comparison and classify pixels in images into various categories based on how closely they resemble the training examples for each type of change (Ye, 2015). In general, supervised change detection techniques produce more accurate and more detailed information about transition between two land-cover types as the training examples help spate spurious changes from the desired changes to be detected. One of the most well-established and widely used detection techniques among the supervised change detection techniques is post-classification comparison. This technique finds change by comparing the thematic classification maps of two dates (Yuan et al., 2005). This method can provide accurate change information which may maybe less affected by external factors such as atmospheric interferences depending on the classes chosen (Asokan and Anitha, 2019).

The choice of a classification method plays a pivotal role in post-classification change detection techniques. The more accurate each map is, the better the resulting change. Consequently, evaluating the effectiveness of various classifiers for land cover classification remains a prominent focus within this field. In 2023, Affonso et al. conducted an examination of changes in land use and land cover (LULC) between 2000 and 2017 within a portion of the Brazilian Amazon Forest. They evaluated several classification methods in their study, which included both parametric approaches such as Mahalanobis distance, maximum likelihood (MLH), and minimum distance, and non-parametric methods like multi-layer perceptron neural network (MLPNN), random forest (RF), and support vector machine (SVM) algorithms. Changes in the landscape were assessed through the post-classification comparison method. The outcomes of their investigation revealed that while maximum likelihood effectively identified errors in specific classes, SVM exhibited a slight advantage when compared to other non-parametric alternatives (Affonso et al., 2023). Dahiya et al. in 2023 proposed a simple

framework-based artificial neural network (ANN) and post-classification comparison to detect the multitemporal changes using both hyperspectral and multispectral datasets and compared their method with well-known RF and SVM post-comparison methods. Their experimental outcomes on both datasets confirmed the effectiveness of ANN post-classification method in the extraction of multitemporal changes followed by RF and SVM post-classification methods (Dahiya et al., 2023). These investigations have demonstrated that the performance of various classifiers can vary based on factors such as data characteristics, the study region, and the context of use. For instance, certain classifiers might be more effective in identifying changes within intricate land use patterns in urban zones, whereas others could be better suited for detecting changes in vegetation or water bodies. Consequently, identifying the most suitable classifiers for extracting distinct urban land use and land cover classes across various timeframes and spatial contexts remains a difficulty, particularly when dealing with datasets that involve multiple time points and sensors (Ouma et al., 2023).

An alternative approach for change detection involves employing difference images as direct input for supervised classifiers to distinguish between changed and unchanged regions. Nonetheless, limited research has been conducted to assess the comparative performance of various classifiers in this context. This approach decreases the time spent on change detection by eliminating the need for land cover classification of multi-temporal images. In 2018, Wang et al. proposed a new change detection scheme that combines multiple features and ensemble learning. They used three kinds of object features including spectral, shape, and texture. Using the image differencing process, a difference image was generated and used as the input for nonlinear supervised classifiers, including k-nearest neighbor (KNN), SVM, extreme learning machine and RF. Finally, the results of multiple classifiers were integrated using an ensemble rule called weighted voting to generate the final change detection result. Their results demonstrated that their proposed approach outperforms four different single supervised classifiers in terms of overall accuracy and generates change detection maps with a higher number of homogeneous regions in urban areas (Wang et al., 2018).

To the best of our knowledge, little research has conducted a comparison between different classifiers in change detection using both post-classification change detection and difference image classification in terms of their efficacy in distinguishing changed and unchanged regions. In this study, six widely employed classifiers—namely KNN, MLH, Gaussian Naïve Bayes (GNB), RF, SVM, and MLPNN—were assessed for their performance in change detection within an urban area using Planet high-resolution satellite imagery. This assessment involves two distinct procedures: post-classification comparison and difference image classification. In addition, one of the most important considerations in supervised classification is to select unbiased training and reference data. In this study, a new unbiased procedure is used to select limited reference data from unchanged and changed areas for change detection.

The rest of the paper is organized as follows. Section 2 introduces the study area and dataset, Section 3 presents our sampling method, post-classification comparison, and difference image classification methods, and Section 4 describes and discusses the results. Section 5 presents our conclusion.

2. Area and Dataset

2.1 Study Area

The study area covers the main part of the City of Kingston located in Eastern Ontario, Canada where the St. Lawrence River flows out of Lake Ontario. This area extends from 76°28′30” W to 76°37′30” W and from 44°12′26” N to 44°17′0.5” N, covering approximately 103 km2. This area is completely flat and its main land covers include forestry areas, agricultural lands, and urban buildings. The elevation range of the study area is from 60 to 145 m above the mean sea level. Google earth satellite image of the study area captured in August 2016 is shown in Figure 1.

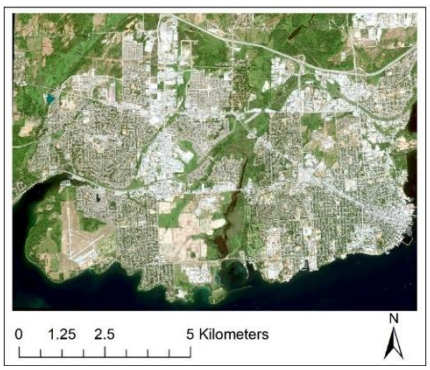

Figure 1. Google earth high resolution satellite image of the Kingston city captured in August 2016.

2.2 Dataset

In order to assess and contrast the effectiveness of various classifiers in detecting urban changes, two remote sensing images were utilized. These images were captured by the PS2 sensor within the Planetscope satellite constellation, offering a resolution of 3 meters. The acquisition dates were September 2016 and July 2020, and each image encompassed four multispectral bands: blue, green, red, and near infrared. Figure 2 presents true-color composite depictions of both images. In an effort to establish reference data, satellite images from Google Earth were employed as supplementary data. These Google Earth images, captured in August 2016 and June 2020, featured a submeter resolution.

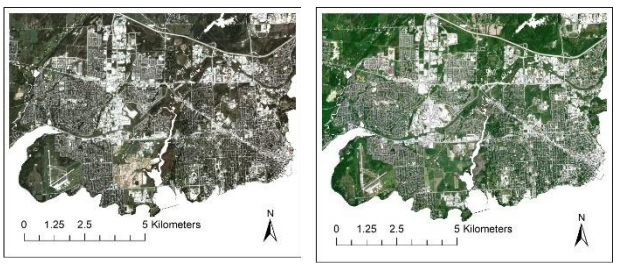

Figure 2. True-color composites of Planet images acquired on a) September 15, 2016, and b) July 16, 2020 of Kingston city.

3. Methodology

As outlined in the introduction, the objective of this study is to compare the performance of six widely employed classifiers in remote sensing using two distinct change detection methods: a) post-classification comparison using classified land cover maps, and b) classification of image band differences to delineate changed and unchanged regions, thus creating a binary change map. To ensure consistency and impartiality, both procedures

employ identical reference data locations for training and testing classifiers and assessing the accuracy of change detection maps. Accordingly, the study introduces a novel unbiased sampling technique that selectively captures a minimal number of reference pixels from both changed and unchanged areas. The procedure of generating training and test data used in this study and the features and steps used in classification are explained in the following sections.

3.1 Sampling method

The efficiency and cost of accuracy assessment in supervised techniques are predominantly influenced by two critical factors: the selected sampling approach and the number of samples, also known as sample size (Chen and Wei, 2009; Jensen, 1996). In order to select spatially and class-unbiased reference pixels in the study area from both changed and unchanged areas, first of all the whole study area was classified into changed and unchanged areas using the RF classifier, one of the most commonly used classifiers in remote sensing for land cover classification (Phan et al., 2020). To this end, regions of interest (ROIs) for different changed and unchanged classes were selected using ENVI software and planet images. The classes used for this section are “change from vegetation to infrastructure (building and roads)”, “change from soil to infrastructure”, “change from vegetation to soil”, “unchanged trees”, “unchanged buildings”, “unchanged roads”, “unchanged soil”, “unchanged vegetation”, and “unchanged shadowy area”. Google Earth images featuring submeter spatial resolution, captured around the same date as the planet images, were additionally employed as supplementary data to enhance the precision of creating ROIs. One of the challenges in ROI creation is shadow areas. To handle this issue, Improved Shadow Index (ISI) , as an effective index in identifying shadows in urban areas, was also used as auxiliary data (Zhou et al., 2021). ISI combine YCbCr color space with a near infrared (NIR) band and is defined by the following formula:

$$\mathrm{ISI} = \frac{\mathrm{SI} + (1 - \mathrm{NIR})}{\mathrm{SI} + (1 + \mathrm{NIR})} \tag{1}$$

in which NIR is the near infrared band and SI is defined as:

$$\mathrm{SI} = \frac{\mathrm{C_b} - \mathrm{Y}}{\mathrm{C_b} + \mathrm{Y}} \tag{2}$$

where Y and Cb are components in the $\mathrm{YC_bC_r}$ model. The $\mathrm{YC_bC_r}$ is defined as follow:

$$\begin{bmatrix} \mathrm{Y} \\ \mathrm{C_b} \\ \mathrm{C_R} \end{bmatrix} = \begin{bmatrix} 0.257 & 0.504 & 0.098 \\ -0.148 & -0.291 & 0.439 \\ 0.439 & -0.368 & -0.071 \end{bmatrix} \begin{bmatrix} \mathrm{R} \\ \mathrm{G} \\ \mathrm{B} \end{bmatrix} + \begin{bmatrix} 16 \\ 128 \\ 128 \end{bmatrix} \tag{3}$$

In the $\mathrm{YC_bC_r}$ model, R,G, and B are red, green, and blue bands, respectively and the Y, Cb, and Cr components are equivalent to the intensity component I, saturation component S, and hue component H in the HSI model (Tsai, 2006). ISI was calculated for both planet images and used as auxiliary data helped to identify shadow areas.

After creating the first ground truth (GT), it was divided randomly into train (60% of GT) and test (40% of GT) data and was used for image classification. Our purpose at this stage was to classify our study area as accurately as possible to changed and unchanged classes and randomly select spatially and class-unbiased samples from both changed and unchanged areas. In this study, red, green, blue and NIR bands along with NDVI and ISI were layer stacked for each image and used for image classification. All the 6 layers at time 1 were subtracted from layers at time 2 and the absolute values of the difference bands were used for image classification using RF classifier. Once the study area was classified into nine distinct classes (comprising three changed and six unchanged classes), the changed classes were merged into a single category labeled as "changed," while the remaining classes were combined into a category labeled as "unchanged." This process yielded a binary change map. The initial classification of the image into various changed and unchanged classes, followed by their integration into a binary map, aimed to enhance the accuracy of the initial change map which increases the speed of reference point generation as the quality of the selected reference points are checked manually.

Based on the Kappa coefficient of test data, the random forest classifier led to an accuracy of 79% for classifying 9 classes and 97% for classifying the images to binary change map when all the changed classes were merged to changed class and the rest of them were merged to unchanged class. The initial GT used in this section (all classes were merged into changed and unchanged for better illustration) and the resulted binary change map are illustrated in Figure 3 (a) and Figure 3 (b), respectively.

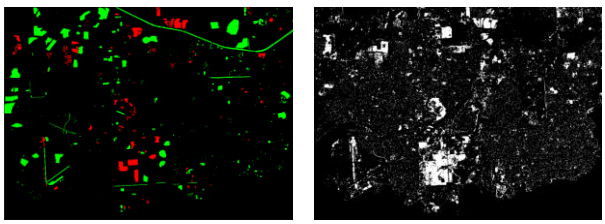

(a) (b)

Figure 3. a) The initial GT of the study area created using Planet images and with the help of google earth images as auxiliary data. Red and green ROIs represent changed and unchanged regions, respectively; b) The binary change map produced using random forest.

Our primary focus when choosing reference points for change detection is to ensure impartiality. Therefore, in the process of selecting reference points based on the computed binary change map, approximately 1000 pixels from changed class and another 1000 pixels from unchanged class were randomly chosen. Figure 4 shows some sample areas and sample points selected randomly from the initial change map. Next, changed and unchanged pixels were inspected carefully and divided into four different groups including true change, false change, true unchanged and false unchanged by the help of auxiliary dataset such as high resolution google earth images and ISIs. The number of reference data used for change detection accuracy assessment are presented in Table 1. It should be noted that all the false changed pixels and false unchanged pixels were considered as unchanged and changed pixels, respectively. This reference data was used to generate training and test data in the process of classifying the study area to change and unchanged areas using image band differences.

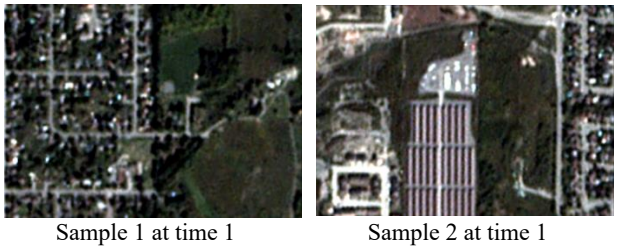

Sample 1 at time 1 Sample 2 at time 1

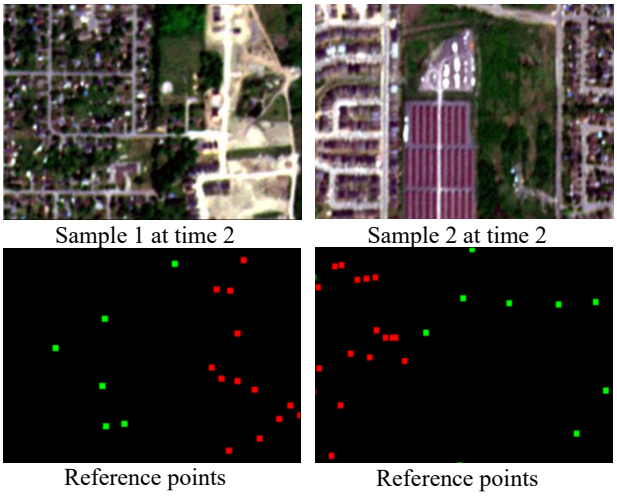

Figure 4. Sample areas and sample points selected randomly as reference data from the change map. Red and green points represent changed and unchanged pixels, respectively. Points labels (changed and unchanged) were revised carefully using auxiliary data.

Type of reference data after visual inspection	True changed pixels	False changed pixels	True unchanged pixels	False unchanged pixels
Number of pixels	796	233	1165	15

Table 1. Number of pixels used as reference data for change detection using planet images.

In order to train the classifiers in the post classification procedure, the same points used as reference data described earlier (~2000 randomly selected points) were utilized, but this time labeled as Constructed area, Asphalt, Vegetation, and Soil classes. To decide about their labels more accurately, auxiliary datasets such as very high resolution google earth images, ISI shadow index, and NDVI were also used. The quantity of reference data utilized for the classification of planet images into distinct land covers is presented in Table 2.

Landcover / Image Date	Constructed	Asphalt	Vegetation	Soil
2016	282	396	1206	325
2020	379	449	901	480

Table 2. Number of pixels used as reference data for landcover classification using planet images.

3.2 Post classification change detection

In the first procedure, Planet image bands captured at two different times, referred to as time 1 and time 2, in addition to NDVI and ISI underwent classification using a selection of six widely recognized classifiers commonly employed in the field of remote sensing. These classifiers encompass three conventional approaches: KNN, MLH, and GNB; as well as three more advanced machine learning oriented techniques: RF, SVM, and MLPNN. A brief description of each classification method is provided below.

3.2.1 KNN Classifier: The KNN classifier is a simple, yet effective algorithm widely used in classification and regression tasks. It assigns a new data point to the most common class among its k nearest neighbors in the feature space. This approach is based on the assumption that similar instances belong to the same class. KNN has been successfully applied remote sensing for various applications, including urban change detection (Fix and Hodges, 1951; Meng et al., 2007).

3.2.2 MLH Classifier: The MLH classifier is a widely used supervised classification method in remote sensing. It calculates the probability of each pixel belonging to a specific class based on the statistical distribution of training samples. It assumes that the spectral values of different classes follow a multivariate normal distribution. The class with the highest likelihood value is assigned to each pixel (Sisodia et al., 2014).

3.2.3 GNB Classifier: The GNB classifier is a probabilistic algorithm used in remote sensing applications. It assumes that the features are independent and normally distributed. It calculates the probability of a sample belonging to a particular class by using Bayes' theorem and assuming that the features are conditionally independent given the class. It has been widely used in remote sensing studies for land cover classification and change detection (Yang et al., 2017; Jamali et al., 2021).

3.2.4 RF Classifier: The RF classifier is a popular machine learning algorithm widely used in various fields, including remote sensing. In the RF classifier, a collection of decision trees is built, and each tree is trained on a random subset of the training data. During classification, each tree in the forest independently predicts the class of a sample, and the class with the most votes is selected as the final prediction. The RF classifier is known for its robustness, ability to handle high-dimensional data, and resistance to overfitting (Pal, 2005).

3.2.5 SVM Classifier: The SVM classifier is another machine learning algorithm commonly used for classification tasks in remote sensing studies. It works by finding an optimal hyperplane in a high-dimensional feature space that separates different classes and minimizes classification error. SVM can handle both linear and nonlinear classification problems by using various kernel functions (Mountrakis et al., 2011).

3.2.6 MLPNN Classifier: The MLPNN constitutes a neural network type characterized by an input layer, one or more hidden layers, and an output layer which are interconnected in a feed-forward manner (Panchal et al., 2011). The MLPNN undergoes a training procedure wherein model parameters are iteratively adjusted to closely align model outputs with observed outputs. The MLPNN classifier is utilized in this study for image classification, with specific parameters tailored for optimal performance. The parameters of the MLPNN, as outlined in Table 3, were determined through experimental exploration aimed at achieving optimal results. MLPNN classifiers have been widely used in remote sensing studies for various applications, including change detection (Dai and Khorram, 1999).

Parameters	Values
Number of hidden layers	4
Number of neurons in each hidden layer	Layer 1: 64 Layer 2: 32 Layer 3: 16 Layer 4: 8

Hidden layers' activation functions	Relu
Output layer's activation functions	Multiclass classification (Post-classification CD): Softmax
	Binary classification (Image differencing CD): Sigmuid
Maximum number of training iteration	1000
Batch size	15
Optimizer	Adam

Table 3. Parameters used in the MLPNN classifier.

The landcovers considered for image classification are on structed area, Road, Vegetation cover and Soil. For training the classifiers, 60% of the reference pixels from both 2016 and 2020 images were selected randomly and used as training data and the rest of them were used as test data. Afterward, land cover classification was performed on both images, followed by a post-classification comparison of the classification maps. By comparing the landcover classes, if the label assigned to a pixel at time 1 was different from its label at time 2, that pixel was considered as changed pixel, otherwise it was considered as unchanged pixel.

3.3 Classification of differencing image for change detection

As the second procedure for the change detection process, the initial step involved subtracting the bands of the planet image at time 1 from their corresponding bands at time 2. Subsequently, the difference of red, green, blue, and NIR bands in addition to NDVI and the ISI were used for image classification. The classes used for image classification are changed and unchanged classes. In this section, the same six classifiers mentioned in Section 2.2 were used for image classification and for consistency, exactly the same pixels used as training and test samples in the first procedure (Post classification change detection), but with change and unchanged labels, were used for training classifiers and testing the accuracy of the change maps, respectively.

4. Results and Discussion

4.1 Post classification change detection

The results of landcover classification and post classification change detection, based on kappa coefficient and the randomly selected reference test data are tabulated in Table 4. The results indicate that, considering landcover classification and evaluating the kappa coefficient of the test data, the MLPNN classifier yielded the highest performance. It was closely followed by the SVM and RF classifiers for both the images captured at time 1 and time 2. All three conventional classifiers yielded lower accuracies compared to neural network, SVM, and RF classifiers. Among the conventional classifiers, the GNB classifier produced the least favourable results, while the accuracy of the MLH classifier closely approached that of the advanced methods.

In terms of post-classification change detection results, the change maps generated by the MLPNN classifier produced the most favourable outcomes with a kappa coefficient of 70.1% on test data, with the RF and SVM classifiers following closely in performance. Among the conventional methods, MLH achieved results comparable to the advanced techniques with a kappa coefficient of 68.4% on test data, while the GNB classifier yielded the least favourable outcomes. The performance of various classifiers in post-classification change detection aligns with their performance in land cover classification, except for SVM and RF classifiers. Specifically, SVM demonstrated superior performance in land cover classification compared to RF, while RF excelled in generating more accurate binary change maps than SVM. The landcover classification maps at time 1 and time 2 created using MLPNN classifier and their corresponding change map are represented in Figure 5.

Classifiers	Landcover classification at time 1	Landcover classification at time 2	Binary post-classification change detection
KNN	0.602	0.574	0.644
MLH	0.663	0.623	0.684
GNB	0.541	0.416	0.668
RF	0. 671	0. 636	0.698
SVM	0. 684	0. 641	0.688
MLPNN	0. 702	0. 642	0.701

Table 4. Accuracies of landcover classification and post classification change maps based on kappa coefficient on test data using different classifiers.

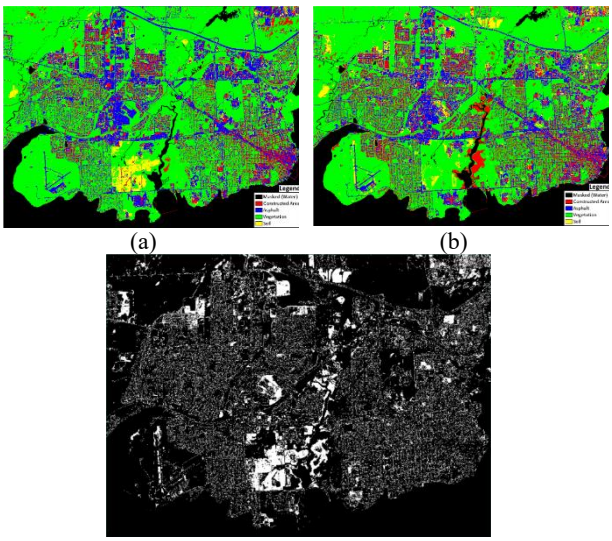

(a) (b)

(c)

Figure 5. a) Land cover classification maps created using MLPNN classifier at a) time 1 and b) time 2 and c) their corresponding change map.

4.2 Classification of differencing image for change detection

As the second procedure for change detection, differences of red, green, blue, and NIR bands in addition to NDVI and ISI at time 1and 2 were used for image classification. As noted earlier, the same reference pixels were used as training and test data to train classifiers and assess the accuracy of change maps for both procedures. The classes used for image classification in this section are just changed and unchanged classes. The results of change detection using different classifiers are presented in Table 5.

As the results show, based on the kappa coefficient of test data, MLPNN classifier led to best results with a kappa coefficient of 87.4% on test data, followed by SVM and RF classifiers. Same as the previous procedure, all the three conventional classifiers

produced lower accuracies than the more advanced classifiers, and the GNB classifier produced the worst results. It is noteworthy that while MLH yielded results comparable to advanced classifiers in post-classification change detection, in the context of the classification of differencing images, the performance of the KNN classifier demonstrated comparable results to the advanced classifiers, with a kappa coefficient of 84.2% on test data which is very close to that of the RF classifier.

Change map created using MLPNN classifier, as the best case in our study, is presented in Figure 6. As the results show, the accuracy of change detection using classification of differencing images (Table 5) is much higher than the post classification method (Table 4) and this is consistent for all the different classifiers used in this study. As a result, the performances of different classifiers for change detection using the second procedure (classification of differencing images) are studied in more detail. For a more in-depth comparison of classifier accuracies, their performances in detecting changed and unchanged areas for some sample regions are investigated. The sample regions include changes from soil to building, changes from vegetation cover to soil, unchanged building, and unchanged soil. The true color images of the sample regions at time 1 and time 2 in addition to their corresponding change maps created by each classifier are presented in Figure 7.

Classifiers	Binary change detection using image differencing process
KNN	0.842
MLH	0.838
GNB	0.8
RF	0. 846
SVM	0. 859
MLPNN	0. 874

Table 5. Accuracies of binary change detection using Image differencing based on kappa coefficient for different classification methods.

Figure 6. Change map created using MLPNN classifier and image differencing.

Based on Figure 7, MLPNN classifier could detect the real changes more accurately than other classifiers. In the sample showing transition from "soil to building", where three new buildings are the primary changes, all classifiers except MLPNN identified some false changes in the vicinity of the buildings. Some of the false changes on the left side of the buildings are because of the shadows created by buildings. Regarding the “vegetation to soil” sample, MLPNN and SVM classifiers could detect the true changes more accurately. The main issue of other classifiers in this case, especially the MLH and GNB classifiers, is missing some parts of truly changed areas. Regarding both unchanged samples, MLPNN and SVM led to the lowest rates of errors in terms of creating false changes while the MLH and GNB classifiers led to the highest rate of commission errors. By comparing RF and KNN classifiers, it can be concluded that KNN classifier could perform even better in these two cases as the RF classifier produced more false changes.

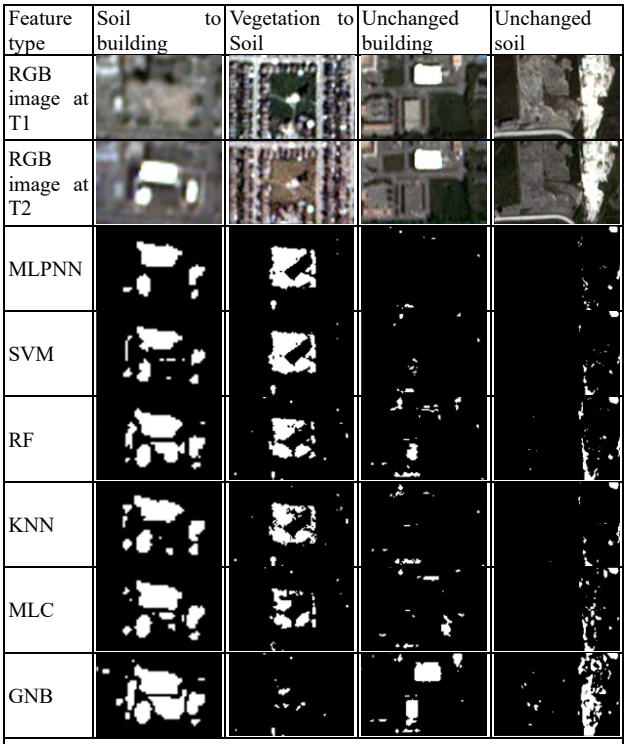

Figure 7. The true color images of the sample regions in addition to change maps created by each classifier method are presented.

5. Conclusion

As the selection of a classification method plays an important role in classification-based change detection techniques, this study aimed to assess the performance of various classification methods, including MLPNN, SVM, RF, GNB, MLH, and KNN, utilizing two distinct change detection techniques: post-classification and classification of image differences. To ensure unbiased training and testing of classifiers, we initially classified the study area using visually interpreted ROIs. Subsequently, we employed the resulting change map to select limited random sample points from both changed and unchanged regions, maintaining consistency in the sample points for both change detection techniques. The accuracy of reference points was carefully checked before using them for training and testing the classifiers.

While the specific ranking of classifier performance varied slightly between the two methods, a consistent pattern emerged. MLPNN consistently delivered the highest accuracy, with RF and SVM closely following as the second or third-best performers in each technique. On the other hand, GNB consistently yielded the least favorable results. Among the conventional methods, MLH in the post-classification technique and KNN in the image differencing method yielded comparable results to the more advanced methods. Notably, our findings revealed that the image differencing technique consistently outperformed post-classification in terms of change detection accuracy across all six classifiers. Additionally, this method demonstrated a significant advantage in terms of reduced processing time and computational resources, making it the

superior choice for binary change detection when compared to post-classification techniques. In future research, we intend to investigate how changes in training sample sizes and image scales affect classification-based change detection when employing a range of diverse classifiers.

References

Affonso, A. A., Mandai, S. S., Portella, T. P., Quintanilha, J. A., Conti, L. A., and Grohmann, C. H.: A Comparison between Supervised Classification Methods: Study Case on Land Cover Change Detection Caused by a Hydroelectric Complex Installation in the Brazilian Amazon, Sustainability, 15, 1309, 2023.

Asokan, A. and Anitha, J.: Change detection techniques for remote sensing applications: A survey, Earth Science Informatics, 12, 143-160, 2019.

Bovolo, F., Marchesi, S., and Bruzzone, L.: A framework for automatic and unsupervised detection of multiple changes in multitemporal images, IEEE Transactions on Geoscience and Remote Sensing, 50, 2196-2212, 2011.

Chen, D. and Wei, H.: The effect of spatial autocorrelation and class proportion on the accuracy measures from different sampling designs, ISPRS Journal of Photogrammetry and Remote Sensing, 64, 140-150, 2009.

Dahiya, N., Gupta, S., and Singh, S.: Qualitative and quantitative analysis of artificial neural network-based post-classification comparison to detect the earth surface variations using hyperspectral and multispectral datasets, Journal of Applied Remote Sensing, 17, 032403-032403, 2023.

Dai, X. L. and Khorram, S.: Remotely sensed change detection based on artificial neural networks, Photogrammetric engineering and remote sensing, 65, 1187-1194, 1999.

Daudt, R. C., Le Saux, B., Boulch, A., and Gousseau, Y.: Urban change detection for multispectral earth observation using convolutional neural networks, IGARSS 2018-2018 IEEE International Geoscience and Remote Sensing Symposium, 2115-2118,

Fernandez-Prieto, D. and Marconcini, M.: A novel partially supervised approach to targeted change detection, IEEE transactions on geoscience and remote sensing, 49, 5016-5038, 2011.

Fix, E. and Hodges, J.: Discriminatory analysis, nonparametric discrimination, 1951.

Hussain, M., Chen, D., Cheng, A., Wei, H., and Stanley, D.: Change detection from remotely sensed images: From pixel-based to object-based approaches, ISPRS Journal of photogrammetry and remote sensing, 80, 91-106, 2013.

Jamali, A., Mahdianpari, M., Brisco, B., Granger, J., Mohammadimanesh, F., and Salehi, B.: Wetland mapping using multi-spectral satellite imagery and deep convolutional neural networks: a case study in Newfoundland and Labrador, Canada, Canadian journal of remote sensing, 47, 243-260, 2021.

Jensen, J.: Thematic information extraction: Image classification, Introductory digital image processing: a remote sensing perspective, 197-256, 1996.

Khan, S. H., He, X., Porikli, F., and Bennamoun, M.: Forest change detection in incomplete satellite images with deep neural networks, IEEE Transactions on Geoscience and Remote Sensing, 55, 5407-5423, 2017.

Li, H., Xiao, P., Feng, X., Yang, Y., Wang, L., Zhang, W., Wang, X., Feng, W., and Chang, X.: Using land long-term data records to map land cover changes in China over 1981–2010, IEEE Journal of Selected Topics in Applied Earth Observations and Remote Sensing, 10, 1372-1389, 2017.

Meng, Q., Cieszewski, C. J., Madden, M., and Borders, B. E.: K nearest neighbor method for forest inventory using remote sensing data, GIScience & Remote Sensing, 44, 149-165, 2007.

Mountrakis, G., Im, J., and Ogole, C.: Support vector machines in remote sensing: A review, ISPRS Journal of Photogrammetry and Remote Sensing, 66, 247-259, 2011.

Mucher, C., Steinnocher, K., Kressler, F., and Heunks, C.: Land cover characterization and change detection for environmental monitoring of pan-Europe, International Journal of Remote Sensing, 21, 1159-1181, 2000.

Ouma, Y. O., Keitsile, A., Nkwae, B., Odirile, P., Moalafhi, D., and Qi, J.: Urban land-use classification using machine learning classifiers: comparative evaluation and post-classification multi-feature fusion approach, European Journal of Remote Sensing, 56, 2173659, 2023.

Pal, M.: Random forest classifier for remote sensing classification, International journal of remote sensing, 26, 217-222, 2005.

Panchal, G., Ganatra, A., Kosta, Y., and Panchal, D.: Behaviour analysis of multilayer perceptrons with multiple hidden neurons and hidden layers, International Journal of Computer Theory and Engineering, 3, 332-337, 2011.

Phan, T. N., Kuch, V., and Lehnert, L. W.: Land cover classification using Google Earth Engine and random forest classifier—The role of image composition, Remote Sensing, 12, 2411, 2020.

Sisodia, P. S., Tiwari, V., and Kumar, A.: Analysis of supervised maximum likelihood classification for remote sensing image, International conference on recent advances and innovations in engineering (ICRAIE-2014), 1-4,

Tan, K., Zhang, Y., Wang, X., and Chen, Y.: Object-based change detection using multiple classifiers and multi-scale uncertainty analysis, Remote Sensing, 11, 359, 2019.

Tsai, V. J.: A comparative study on shadow compensation of color aerial images in invariant color models, IEEE transactions on geoscience and remote sensing, 44, 1661-1671, 2006.

Usman, M., Liedl, R., Shahid, M., and Abbas, A.: Land use/land cover classification and its change detection using multi-temporal MODIS NDVI data, Journal of Geographical sciences, 25, 1479-1506, 2015.

Wang, X., Liu, S., Du, P., Liang, H., Xia, J., and Li, Y.: Object-based change detection in urban areas from high spatial resolution images based on multiple features and ensemble learning, Remote Sensing, 10, 276, 2018.

Yang, J., Ye, Z., Zhang, X., Liu, W., and Jin, H.: Attribute weighted Naive Bayes for remote sensing image classification based on cuckoo search algorithm, 2017 International Conference on Security, Pattern Analysis, and Cybernetics (SPAC), 169-174,

Ye, S.: Improved Framework for Monitoring Land-cover Changes by Using Remote Sensing Technology: From unsupervised and supervised, to targeted approaches, the School of Environmental Studies, Queen's University, 113 pp., 2015.

Yuan, F., Sawaya, K. E., Loeffelholz, B. C., and Bauer, M. E.: Land cover classification and change analysis of the Twin Cities (Minnesota) Metropolitan Area by multitemporal Landsat remote sensing, Remote sensing of Environment, 98, 317-328, 2005.

Zhou, T., Fu, H., Sun, C., and Wang, S.: Shadow detection and compensation from remote sensing images under complex urban conditions, Remote Sensing, 13, 699, 2021.